The neutrino mass bound from WMAP-3, the baryon acoustic peak, the SNLS supernovae and the Lyman-α forest

Ariel Goobar[1], Steen Hannestad[2], Edvard Mörtsell[3], Huitzu Tu[2]

[1] Department of Physics, Stockholm University, SE-106 91 Stockholm, Sweden

[2] Department of Physics and Astronomy, University of Aarhus,
Ny Munkegade, DK-8000 Aarhus C, Denmark

[3] Department of Astronomy, Stockholm University, SE-106 91 Stockholm, Sweden

Abstract. We have studied bounds on the neutrino mass using new data from the WMAP 3 year data, the Sloan Digital Sky Survey measurement of the baryon acoustic peak, the Type Ia supernovae from SNLS, and the Lyman-α forest. We find that even in the most general models with a running spectral index where the number of neutrinos and the dark energy equation of state are allowed to vary, the 95% C.L. bound on the sum of neutrino masses is $\sum m_\nu \leq 0.62$ eV (95% C.L.), a bound which we believe to be robust. In the more often used constrained analysis with $N_\nu = 3$, $w = -1$, and $\alpha_s = 0$, we find a bound of 0.48 eV without using the Lyman-α data. If Lyman-α data is used, the bound shrinks to $\sum m_\nu \leq 0.2 - 0.4$ eV (95% C.L.), depending strongly on the Lyman-α analysis used.

1. Introduction

In the past few years a new standard model of cosmology has been established in which most of the energy density of the Universe is made up of a component with negative pressure, generically referred to as dark energy. The simplest form of dark energy is the cosmological constant, Λ, which obeys $P_\Lambda = -\rho_\Lambda$. This model provides an amazingly good fit to all observational data with relatively few free parameters and has allowed for stringent constraints on the basic cosmological parameters.

The precision of the data is now at a level where observations of the cosmic microwave background (CMB), the large scale structure (LSS) of galaxies, and Type Ia supernovae (SNIa) can be used to probe important aspects of particle physics such as neutrino properties. Conversely, cosmology is now also at a level where unknowns from the particle physics side can significantly bias estimates of cosmological parameters.

The combination of all currently available data from neutrino oscillation experiments suggests two important mass differences in the neutrino mass hierarchy. The solar mass difference of $\Delta m_{12}^2 \simeq 8 \times 10^{-5}$ eV^2 and the atmospheric mass difference $\Delta m_{23}^2 \simeq 2.2 \times 10^{-3}$ eV^2 [1]. In the simplest case where neutrino masses are hierarchical these results suggest that $m_1 \sim 0$, $m_2 \sim \Delta m_{\mathrm{solar}}$, and $m_3 \sim \Delta m_{\mathrm{atmospheric}}$. If the hierarchy is inverted one instead finds $m_3 \sim 0$, $m_2 \sim \Delta m_{\mathrm{atmospheric}}$, and $m_1 \sim \Delta m_{\mathrm{atmospheric}}$. However, it is also possible that neutrino masses are degenerate, $m_1 \sim m_2 \sim m_3 \gg \Delta m_{\mathrm{atmospheric}}$. Since oscillation probabilities depend only on squared mass differences, Δm^2, such experiments have no sensitivity to the absolute value of neutrino masses, and if the masses are degenerate, oscillation experiments are not useful for determining the absolute mass scale.

Instead, it is better to rely on kinematical probes of the neutrino mass. Using observations of the CMB and the LSS of galaxies it has been possible to constrain masses of standard model neutrinos. The bound can be derived because massive neutrinos contribute to the cosmological matter density, but they become non-relativistic so late that any perturbation in neutrinos up to scales around the causal horizon at matter-radiation equality is erased, i.e. the kinematics of the neutrino mass influences the growth of structure in the Universe. Quantitatively, neutrino free streaming leads to a suppression of fluctuations on small scales relative to large by roughly $\Delta P/P \sim -8\Omega_\nu/\Omega_m$ [2]. The density in neutrinos is related to the number of massive neutrinos and the neutrino mass by

$$\Omega_\nu h^2 = \frac{\sum m_\nu}{93.2\,\mathrm{eV}} = \frac{N_\nu m_\nu}{93.2\,\mathrm{eV}}, \tag{1}$$

where h is the Hubble parameter in units of 100 km s^{-1} Mpc^{-1} and all neutrinos are assumed to have the same mass. Such an effect would be clearly visible in LSS measurements, provided that the neutrino mass is sufficiently large, and a likelihood analysis based on the standard ΛCDM model with neutrino mass as an added parameter in general provides a bound for the sum of neutrino masses of roughly $\sum m_\nu \lesssim 0.5 - 1$ eV, depending on exactly which data is used [4–14].

This should be compared to the present laboratory bound from ^{3}H beta decay found in the Mainz experiment, $m_{\nu_e} = \left(\sum_i |U_{ei}|^2 m_i^2\right)^{1/2} \leq 2.3$ eV [15]. It should also be contrasted to the claimed signal for neutrinoless double beta decay in the Heidelberg-Moscow experiment [16–18], which would indicate a value of 0.1-0.9 eV for the relevant combination of mass eigenstates, $m_{ee} = \left|\sum_j U_{ej}^2 m_{\nu_j}\right|$. Some papers claim that the cosmological neutrino mass bound is already incompatible with this measurement.

However, those claims are based on a relatively limited parameter space. Using a much more complicated model with a non-power law primordial power spectrum it is possible to accomodate large neutrino masses, provided that SNIa data is discarded [40]. It was recently shown that there is a strong degeneracy between neutrino mass and the equation of state of the dark energy component when CMB, LSS, and SNIa data is considered. The reason is that when the neutrino mass is increased, the matter density must be increased accordingly in order not to conflict with LSS data. This is normally excluded when the dark energy is in the form of a cosmological constant. However, when the equation of state parameter of the dark energy fluid, w, is taken to be a free parameter, an increase in the matter density can be compensated by a decrease in w to more negative values.

Here we study how the degeneracy can be broken by the addition of information provided by the measurement of the baryon acoustic beak in the Sloan Digital Sky Survey data and the distances to Type Ia supernovae provided by the SNLS data. We also study constraints derived from combining all available cosmological data, including the measurement of the small scale matter power spectrum from the Lyman-α forest.

In the next section we discuss the cosmological data used, in section 3 numerical results from the likelihood analysis are provided, and finally section 4 contains a discussion.

2. Cosmological data

In order to probe the neutrino mass we have used some of the most recent precision CMB, LSS and SNIa data.

2.1. Type Ia supernovae.

Observations of SNIa over a wide redshift range to determine cosmological distances is perhaps the most direct way to probe the energy content of the universe [19] and have lead to a major paradigm shift in cosmology [20–25]. While extremely succesful at showing the need for *dark energy* to explain the derived distances, these data sets are plagued by systematic uncertainties (e.g. dust extinction corrections, K-corrections, calibration uncertainties, non-Ia contamination, Malmquist bias, weak lensing uncertainties, etc.) rendering them non-optimal for precision tests on w. However, the situation has improved since the start of a dedicated experiment, the SuperNova Legacy Survey (SNLS) at CFHT. Thanks to the multi-band, rolling search

technique, extensive spectroscopic follow-up at the largest ground based telescopes and careful calibration, this data-set is arguably the best high-z SNIa compilation to date, indicated by the very tight scatter around the best fit in the Hubble diagram and the careful estimate of systematic uncertainties by Astier et al., (2006) [26]. The first year data of the SNLS collaboration includes 71 high redshift SNIa in the redshift range $z = [0.2, 1]$ and 44 low redshift SNIa compiled from the literature but analysed in the same manner as the high-z sample. We thus make only use of this new SNIa data set to minimize the effects from systematic uncertainties in our analysis.

It should be noted that combining the results in Ref. [26] with the Gold sample of Riess et al. (2004) [25] as done in, e.g. Refs. [3] and [62] is not straight forward. First, the two data-sets use the same low-redshift samples to anchor the Hubble diagram and are thus not independent. Second, there are systematic differences in the way the SNe are analysed, e.g. with respect to reddening corrections. In a combined analysis, this would have to be adressed.

2.2. Large Scale Structure (LSS).

Any large scale structure survey measures the correlation function between galaxies. In the linear regime where fluctuations are Gaussian the fluctuations can be described by the galaxy-galaxy power spectrum alone, $P(k) = |\delta_{k,gg}|^2$. In general, the galaxy-galaxy power spectrum is related to the matter power spectrum via a bias parameter, $b^2 \equiv P_{gg}/P_m$. In the linear regime, the bias parameter is approximately constant, so up to a normalization constant, P_{gg} does measure the matter power spectrum.

At present there are two large galaxy surveys of comparable size, the Sloan Digital Sky Survey (SDSS) [27, 28] and the 2dFGRS (2 degree Field Galaxy Redshift Survey) [29]. Once the SDSS is completed in 2006 it will be significantly larger and more accurate than the 2dFGRS. In the present analysis we use data from both surveys. In the data analysis we use only data points on scales larger than $k = 0.15h/\text{Mpc}$ in order to avoid problems with non-linearity.

2.3. Baryon acoustic oscillations (BAO).

The acoustic oscillations at the time of CMB decoupling should be imprinted also on the low-redshift clustering of matter and manifest themselves as a single peak in the galaxy correlation function at $\sim 100h^{-1}$ Mpc separation. Because of the large scale and small amplitude of the peak, surveys of very large volumes are necessary in order to detect the effect.

A power spectrum analysis of the final 2dFGRS data shows deviations from a smooth curve at the scales expected for the acoustic oscillations. The signature is much smaller than the corresponding acoustic oscillations in the CMB but can be used to reject the case of no baryons at 99% C.L. [30].

The SDSS luminous red galaxy (LRG) sample contains 46,748 galaxies with spectroscopic redshifts $0.16 < z < 0.47$ over 3816 square degrees. Even though the

number of galaxies is less than the 2dFGRS or the main SDSS samples, the large survey volume $(0.72h^{-3}\ \text{Gpc}^3)$ makes the LRG sample better suited for the study of structure on the largest scales. The LRG correlation function shows a significant bump at the expected scale of ~ 150 Mpc which, combined with the detection of acoustic oscillations in the 2dFGRS power spectrum, confirms our picture of LSS formation between the epoch of CMB decoupling and the present.

For a given cosmology, we can predict the correlation function (up to an amplitude factor which is marginalized over) and compare with the observed LRG data. The observed position of the peak will depend on the physical scale of the clustering and the distance relation used in converting the observed angular positions and redshifts to positions in physical space. The characteristic physical scale of the acoustic oscillations is given by the sound horizon at the time of CMB decoupling and depends most strongly on the combination $\Omega_m h^2$. The conversion between positions in angular and redshift space to positions in physical space will cause the observed correlation scale to depend on the distance combination

$$D_V(z) = \left[D_M(z)^2 \frac{cz}{H(z)} \right]^{1/3} , \qquad (2)$$

where $H(z)$ is the Hubble parameter and $D_M(z)$ is the comoving angular diameter distance.

Our approach to fit the data has been to calculate the matter power spectrum for a given model, then Fourier transforming it to obtain the 2-point correlation function, $\xi(r)$. This correlation function has been fitted to the SDSS data using the full covariance matrix given by [31].

In terms of the simple parametrization provided by [31] in terms of the parameter

$$A \equiv D_V(z) \frac{\sqrt{\Omega_m H_0^2}}{zc} , \qquad (3)$$

we find that the SDSS constraint can approximately be written as

$$A = 0.469 \left(\frac{n}{0.98} \right)^{-0.35} (1 + 0.94 f_\nu) \pm 0.017 , \qquad (4)$$

where $f_\nu = \Omega_\nu / \Omega_m$.

2.4. The Lyman-α forest.

Measurements of the flux power spectrum of the Lyman-α forest has been used to measure the matter power spectrum on small scales at large redshift. By far the largest sample of spectra comes from the SDSS survey. In Ref. [33] this data was carefully analyzed and used to constrain the linear matter power spectrum. The derived amplitude is $\Delta^2(k = 0.009\ \text{km s}^{-1}, z = 3) = 0.452^{+0.07}_{-0.06}$ and the effective spectral index is $n_{\text{eff}} = -2.321^{+0.06}_{-0.05}$. The result has been derived using a very elaborate model for the local intergalactic medium, including full N-body simulations. It has been shown that using the Lyman-α data does strengthen the bound on neutrino mass significantly.

However the question remains as to the level of systematic uncertainty in the result. The same data has been reanalyzed by Seljak et al. [62] and Viel et al. [63–65], with somewhat different results. The normalization found in Refs. [63–65] is lower than that found by Ref. [33] which has significant influence on the inferred neutrino mass bound.

Our Lyman-α analysis uses only the effective parameters $\Delta^2(k)$ and n_s. The resulting bound on m_ν using these parameters was shown in Ref. [12] to be very similar to those obtained in a full analysis. Furthermore we stress that using these parameters makes it very simple to test the influence on different assumptions about the Lyman-α data on the neutrino mass bound.

2.5. Cosmic Microwave Background (CMB).

The temperature fluctuations are conveniently described in terms of the spherical harmonics power spectrum $C_{T,l} \equiv \langle |a_{lm}|^2 \rangle$, where $\frac{\Delta T}{T}(\theta, \phi) = \sum_{lm} a_{lm} Y_{lm}(\theta, \phi)$. Since Thomson scattering polarizes light, there are also power spectra coming from the polarization. The polarization can be divided into a curl-free (E) and a curl (B) component, yielding four independent power spectra: $C_{T,l}$, $C_{E,l}$, $C_{B,l}$, and the T-E cross-correlation $C_{TE,l}$.

The WMAP experiment has reported data on $C_{T,l}$ and , $C_{EE,l}$, and $C_{TE,l}$ as described in Refs. [3, 34, 35] . We have performed our likelihood analysis using the prescription given by the WMAP collaboration [3, 34, 35].

We furthermore use the newly published results from the Boomerang experiment [37–39] which has measured significantly smaller scales than WMAP.

3. Likelihood analysis

Using the presently available precision data we have performed a likelihood analysis for the neutrino mass.

As our framework we choose a flat dark energy model with the following free parameters: Ω_m, the matter density, the curvature parameter, Ω_b, the baryon density, w, the dark energy equation of state, H_0, the Hubble parameter, n_s, the spectral index of the initial power spectrum, α_s, the running of the primordial spectral index, N_ν, the effective number of neutrino species, and τ, the optical depth to reionization. Finally, the normalization, Q, of the CMB data, and the bias parameter b are used as free parameters. The dark energy density is given by the flatness condition $\Omega_{\rm DE} = 1 - \Omega_m - \Omega_\nu$. Including the neutrino mass our benchmark model has 11 free parameters. We also test more restricted parameter spaces in order to probe parameter degeneracies.

The priors we use are given in Table 1. The prior on the Hubble constant comes from the HST Hubble key project value of $h_0 = 0.72 \pm 0.08$ [36], where $h_0 = H_0/100 \, {\rm km \, s^{-1} \, Mpc^{-1}}$.

When calculating constraints, the likelihood function is found by minimizing χ^2 over all parameters not appearing in the fit (i.e. over all other parameters than m_ν).

parameter	prior	
$\Omega = \Omega_m + \Omega_{\mathrm{DE}} + \Omega_\nu$	1	Fixed
Ω_m	0–1	Top hat
h	0.72 ± 0.08	Gaussian [36]
$\Omega_b h^2$	0.014–0.040	Top hat
N_ν	$0 - 10$	Top hat
w_{DE}	$-2.5 - -0.5$	Top hat
n_s	0.6–1.4	Top hat
α_s	$-0.5 - 0.5$	Top Hat
τ	0–1	Top hat
Q	—	Free
b	—	Free
$\sum m_\nu$	—	Fitted over

Table 1. The different priors on parameters used in the likelihood analysis.

3.1. Results

In Fig. 1 we show the one dimensional likelihood function for the neutrino mass for various different data sets, using the full 11-dimensional parameter space.

By far the most conservative is for the case which includes only CMB, LSS, and SN-Ia data. Because the parameter space is larger than the one used in Ref. [41], the constraint of 1.72 eV is, however, stronger because the addition of new WMAP-3 data breaks some of the degeneracy ‡. It should be noted though that the bound is weaker than the one shown in Fig. 18 of Ref. [3]. The main reason for this is most likely that N_ν and α_s is allowed to vary.

When the BAO data is added it has the effect of essentially breaking the degeneracy between m_ν and w. The reason is that the BAO measurement is almost orthogonal to the SNIa measurement in the $[\Omega_m, w]$-plane. For this case the bound shrinks to 0.62 eV, a factor of three improvement.

We also test the inclusion of SDSS Lyman-α data in the fit. When BAO data is not included the Lyman-α data itself does break some of the degeneracy, to a level where the formal bound is 0.83 eV. Including both BAO and Lyman-α data does lead to a significant improvement, the combined bound being 0.49 eV at 2σ.

It is interesting to see how this bound compares with the value obtained in the standard ΛCDM$+m_\nu$ parameter space (which has 8 parameters). Including the BAO data we find an upper bound of 0.48 eV, and with the SDSS Lyman-α data we find 0.35 eV. Combining all data leads to a bound of 0.27 eV. It should be noted that this bound is somewhat weaker than what is found in Ref. [62], presumably because of the

‡ Note, however, that if only WMAP-3 data is used, the inferred bound of 2 eV [42] is almost identical to what is found from WMAP-1. This means that if used alone WMAP-3 does not add significant new information

Data	m_ν (95% C.L.)
1: CMB, LSS, SNIa	1.72 eV
2: CMB, LSS, SNIa, BAO	0.62 eV
3: CMB, LSS, SNIa, Ly-α	0.83 eV
4: CMB, LSS, SNIa, BAO, Ly-α	0.49 eV

Table 2. Best fit χ^2 values for the four different analyses presented in Fig. 1, in all cases based on the full 11-dimensional parameter space.

Data	m_ν (95% C.L.)
1: CMB, LSS, SNIa	0.70 eV
2: CMB, LSS, SNIa, BAO	0.48 eV
3: CMB, LSS, SNIa, Ly-α	0.35 eV
4: CMB, LSS, SNIa, BAO, Ly-α	0.27 eV

Table 3. Best fit χ^2 values for the three different analyses presented in Fig. 2, in all cases based on the restricted 8-dimensional parameter space with $N_\nu = 3$, $w = -1$, and $\alpha_s = 0$.

new treatment of Lyman-α in Ref. [62].

The strength of the bound including Lyman-α therefore depends crucially on the assumed uncertainty in the measurement of $\Delta^2(k)$. We have not used the most recent analysis of the SDSS data by Seljak et al. [62], but in order to compare roughly with their result we have added Lyman-α data that mimics what is shown in their Fig. 1. For this model we find a bound of 0.20 eV, in good agreement with their result of 0.17 eV.

However, we also note that using the Lyman-α result from Viel et al. [63–65] which, when combined with WMAP-3, has a best-fit normalization (note that this is mainly due to the fact that the high resolution Lyman-α data used in Refs. [63–65] has larger error bars) about 2σ lower than in Ref. [62], would lead to a different bound on $\sum m_\nu$. To test this we have also run a likelihood analysis using the Viel et al. data on $\Delta^2(k)$ and found a bound of 0.40 eV. This is the limit we inferred by using the derived cosmological parameters from the analysis of the SDSS data of [63–65], which consists of a Taylor expansion of the flux power around a best fit model (SDSS-d in their tables). With this analysis the bound from Lyman-α adds relatively little information to that obtained from BAO data. We show the χ^2 curves for this analysis in Fig. 3.

This result leads to the inevitable conclusion that while the Lyman-α data holds the potential to provide crucial information on the neutrino mass, there seem to be unresolved systematic issues related to the conversion of the measured flux power spectrum to $\Delta^2(k)$. Any bound derived from the use of the Lyman-α power spectrum should therefore be treated with some caution. This is especially true since in the Seljak et al. [62] analysis there is a tension between the WMAP and Lyman-α normalization on
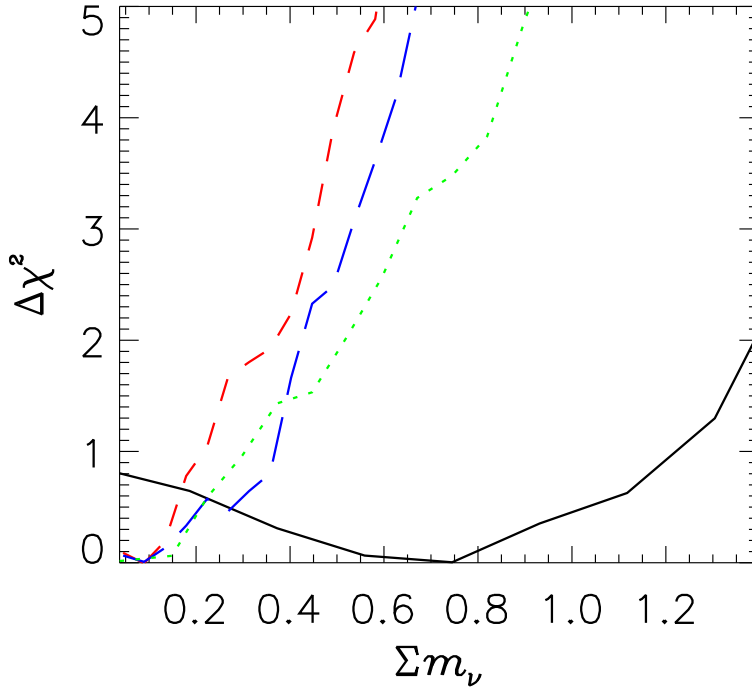
Figure 1. The value of $\Delta\chi^2$ as a function of $\sum m_\nu$ for various different data sets used for the full 11-dimensional parameter space. The curves are identical to the cases described in Table 2: The full curve is case 1, the long-dashed is case 2, the dotted is case 3, and the dashed is case 4.

small scales of more than 2σ. While this could be statistical in nature, the difference with respect to the Viel et al. [65] analysis of the same data suggests a possible systematic origin.

4. Discussion

We have calculated the bound on the sum of light neutrino masses from a combination of the most recent cosmological data. If only CMB, LSS, and SNIa data is used, we find a strong degeneracy between $\sum m_\nu$, N_ν, and w which severely limits the ability of this data to constrain the neutrino mass. However, once data from the SDSS measurement of the baryon acoustic peak is included, this degeneracy is broken because it measures Ω_m and w very precisely. The derived bound and best fit model is compatible with what can be derived from observations of the Lyman-α forest, but is likely much less affected by systematics. The bound is $\sum m_\nu \lesssim 0.6$ eV even for a very general 11 parameter cosmological model. If data from the Lyman-α forest is added, the bound is $\sum m_\nu < 0.2 - 0.4$ eV (95% C.L.), depending on the specific Lyman-α analysis used.

Beyond SDSS, future galaxy redshift surveys will achieve a larger effective volume and go to higher redshifts (see for instance Ref. [43]). The prospects for them to constrain m_ν have been studied in e.g. Refs. [44, 45]. With the help of the BAO measurement, the angular diameter distance and the Hubble parameter $H(z)$ can be measured to percent
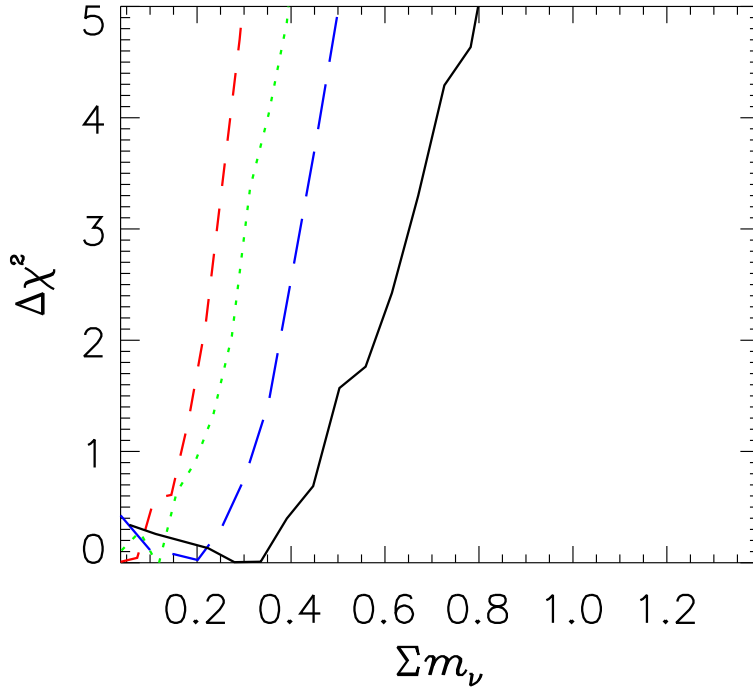
Figure 2. The value of $\Delta\chi^2$ as a function of $\sum m_\nu$ for various different data sets used for the restricted 8-dimensional parameter space with $N_\nu = 3$, $w = -1$, and $\alpha_s = 0$. The curves are identical to the cases described in Table 3: The full curve is case 1, the long-dashed is case 2, the dotted is case 3, and the dashed is case 4.
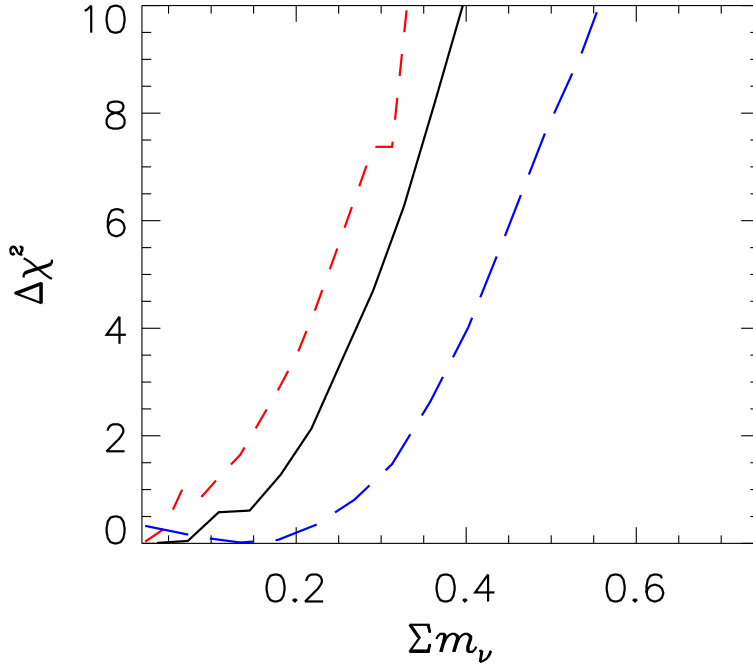

Figure 3. The value of $\Delta\chi^2$ as a function of $\sum m_\nu$ for the restricted 8-dimensional parameter space with $N_\nu = 3$, $w = -1$, and $\alpha_s = 0$ for different assumptions about the Lyman-α data. The full line is for the Ref. [33] data, the dashed is for the approximate analysis with the data in Ref. [62], and the long-dashed is for the data in Ref. [65].

level. This enables w to be determined within $\sim 10\%$ [46–48], breaking the $m_\nu - w$ degeneracy.

Another powerful probe in the future is weak gravitational lensing. It traces directly the mass distribution in a wide range of scales, and thus does not suffer from the light-to-mass bias in large scale structure surveys, while still being sensitive to effects from neutrino early free-streaming. Cosmic shear measurement with tomographic redshift binning of sources galaxies is particularly effective in constraining dark energy parameters. The degeneracy between m_ν and w can then be broken in a similar way as BAO does. Systematics herein arise from photometric redshift uncertainties and shear calibration errors, which are expected to be under control to the required accuracy. The major uncertainty comes from estimating the nonlinear part of the matter power spectrum [49, 50]. It is found that future ground- and space-based surveys such as CFTHLS [55], SNAP [56] and LSST [57], combined with future CMB measurement from the Planck Surveyor [58], can constrain neutrino mass to $\sigma(\sum m_\nu) = 0.025 - 0.1$ eV [51, 52].

CMB photons from the last scattering surface at $z \approx 1100$ are also deflected by the large scale structure at $z \lesssim 3$. Extracting the weak lensing information encoded in the CMB signal will significantly enhance the sensitivity of CMB experiments to small neutrino mass [53, 54]. The forecast error $\sigma(\sum m_\nu)$ obtained in Ref. [53] is ~ 0.15 eV for Planck and SAMPAN [59], and 0.035 eV for the future Inflation Probe project [60]. To summarize, we expect near future cosmological observations to pin down the total neutrino mass to a precision better than 0.1 eV, the level of the inverted hierarchy.

Acknowledgments

References

[1] M. Maltoni, T. Schwetz, M. A. Tortola and J. W. F. Valle, arXiv:hep-ph/0405172.

[2] W. Hu, D. J. Eisenstein and M. Tegmark, Phys. Rev. Lett. **80** (1998) 5255.

[3] D. N. Spergel *et al.*, arXiv:astro-ph/0603449.

[4] S. Hannestad, JCAP **0305** (2003) 004 [astro-ph/0303076].

[5] O. Elgaroy and O. Lahav, JCAP **0304** (2003) 004 [astro-ph/0303089].

[6] S. W. Allen, R. W. Schmidt and S. L. Bridle, Mon. Not. Roy. Astron. Soc. **346**, 593 (2003) [arXiv:astro-ph/0306386].

[7] V. Barger, D. Marfatia and A. Tregre, Phys. Lett. B **595**, 55 (2004) [arXiv:hep-ph/0312065].

[8] S. Hannestad and G. Raffelt, JCAP **0404**, 008 (2004) [arXiv:hep-ph/0312154].

[9] P. Crotty, J. Lesgourgues and S. Pastor, Phys. Rev. D **69**, 123007 (2004) [arXiv:hep-ph/0402049].

[10] S. Hannestad, New J. Phys. **6**, 108 (2004) [arXiv:hep-ph/0404239].

[11] U. Seljak *et al.*, Phys. Rev. D **71**, 103515 (2005) [arXiv:astro-ph/0407372].

[12] G. L. Fogli, E. Lisi, A. Marrone, A. Melchiorri, A. Palazzo, P. Serra and J. Silk, arXiv:hep-ph/0408045.

[13] S. Hannestad, arXiv:hep-ph/0409108.

[14] M. Tegmark, hep-ph/0503257.

[15] C. Kraus *et al.* European Physical Journal C (2003), proceedings of the EPS 2003 - High Energy Physics (HEP) conference.

[16] H. V. Klapdor-Kleingrothaus, A. Dietz, H. L. Harney and I. V. Krivosheina, Mod. Phys. Lett. A **16**, 2409 (2001) [arXiv:hep-ph/0201231].

[17] H. V. Klapdor-Kleingrothaus, I. V. Krivosheina, A. Dietz and O. Chkvorets, Phys. Lett. B **586**, 198 (2004) [arXiv:hep-ph/0404088].

[18] H. Volker Klapdor-Kleingrothaus, arXiv:hep-ph/0512263.

[19] A. Goobar and S. Perlmutter, Astrophys. J, **450**, 14 (1995)

[20] S. Perlmutter et al., Astrophys. J, **517**, 565 (1999)

[21] B. P. Schmidt, et al. Astrophys. J, **507**, 46, (1998)

[22] A. G. Riess, et al. Astron. J,**116**, 1009, (1998)

[23] R. Knop et al., Astrophys. J, **598**, 102 (2003)

[24] J. L. Tonry, et al., , 594, 1 Astrophys. J, **594**, 1, (2003)

[25] A. G. Riess, et al. Astrophys. J, **607**, 665, (2004)

[26] P. Astier, P. et al, Astron. and Astrophys. **447**, 31, (2006)

[27] M. Tegmark *et al.* [SDSS Collaboration], Astrophys. J. **606**, 702 (2004) [arXiv:astro-ph/0310725].

[28] M. Tegmark *et al.* [SDSS Collaboration], Phys. Rev. D **69**, 103501 (2004) [arXiv:astro-ph/0310723].

[29] M. Colless *et al.*, astro-ph/0306581.

[30] Cole, S., et al. 2005 *Monthly Notices of the Royal Astronomical Society* **362** 505

[31] Eisenstein, D. J., et al. 2005 *Astrophysical Journal* **633** 560

[32] Bond, J. R., Efstathiou, G., & Tegmark, M. 1997 *Monthly Notices of the Royal Astronomical Society* **291** L33

[33] P. McDonald *et al.*, Astrophys. J. **635**, 761 (2005) [arXiv:astro-ph/0407377].

[34] G. Hinshaw *et al.*, arXiv:astro-ph/0603451.

[35] L. Page *et al.*, arXiv:astro-ph/0603450.

[36] W. L. Freedman *et al.*, Astrophys. J. Lett. **553**, 47 (2001).

[37] W. C. Jones *et al.*, arXiv:astro-ph/0507494.

[38] F. Piacentini *et al.*, arXiv:astro-ph/0507507.

[39] T. E. Montroy *et al.*, arXiv:astro-ph/0507514.

[40] A. Blanchard, M. Douspis, M. Rowan-Robinson and S. Sarkar, Astron. Astrophys. **412**, 35 (2003)

[41] S. Hannestad, Phys. Rev. Lett. **95**, 221301 (2005) [arXiv:astro-ph/0505551].

[42] M. Fukugita, K. Ichikawa, M. Kawasaki and O. Lahav, arXiv:astro-ph/0605362.

[43] D. Eisenstein, arXiv:astro-ph/0301623.

[44] J. Lesgourgues, S. Pastor and L. Perotto, Phys. Rev. D **70** (2004) 045016 [arXiv:hep-ph/0403296].

[45] M. Takada, E. Komatsu and T. Futamase, arXiv:astro-ph/0512374.

[46] H. J. Seo and D. J. Eisenstein, Astrophys. J. **598** (2003) 720 [arXiv:astro-ph/0307460].

[47] T. Matsubara, Astrophys. J. **615**, 573 (2004) [arXiv:astro-ph/0408349].

[48] Y. Wang, arXiv:astro-ph/0601163.

[49] Mon. Not. Roy. Astron. Soc. **341** (2003) 1311 [arXiv:astro-ph/0207664].

[50] A. Cooray and R. Sheth, Phys. Rept. **372**, 1 (2002) [arXiv:astro-ph/0206508].

[51] Y. S. Song and L. Knox, arXiv:astro-ph/0312175.

[52] S. Hannestad, H. Tu and Y. Y. Wong, work in preparation.

[53] J. Lesgourgues, L. Perotto, S. Pastor and M. Piat, arXiv:astro-ph/0511735.

[54] M. Kaplinghat, L. Knox and Y. S. Song, Phys. Rev. Lett. **91** (2003) 241301 [arXiv:astro-ph/0303344].

[55] http://www.cfht.hawaii.edu/Science/CFHLS/

[56] http://snap.lbl.gov/

[57] http://www.lsst.org/lsst_home.shtml

[58] http://www.rssd.esa.int/index.php?project=Planck

[59] F. R. Bouchet *et al.*, astro-ph/0510423

[60] http://cfa-www.harvard.edu/cip/

[61] U. Seljak and M. Zaldarriaga, Astrophys. J. **469** (1996) 437 See also the CMBFAST website at http://www.cmbfast.org

[62] U. Seljak, A. Slosar and P. McDonald, arXiv:astro-ph/0604335.

[63] M. Viel, M. G. Haehnelt and V. Springel, Mon. Not. Roy. Astron. Soc. **367**, 1655 (2006) [arXiv:astro-ph/0504641].

[64] M. Viel and M. G. Haehnelt, Mon. Not. Roy. Astron. Soc. **365**, 231 (2006) [arXiv:astro-ph/0508177].

[65] M. Viel, M. G. Haehnelt and A. Lewis, arXiv:astro-ph/0604310.